arXiv:nucl-th/0405032v1 12 May 2004

Pairing transition of nuclei at finite temperature

K. Kaneko [a] and M. Hasegawa [b]

[a] *Department of Physics, Kyushu Sangyo University, Fukuoka 813-8503, Japan*

[b] *Laboratory of Physics, Fukuoka Dental College, Fukuoka 814-0193, Japan*

Abstract

Pairing transition at finite temperature was investigated by the shell model and BCS calculations. The definitive signature of pairing transition is identified by a "transition temperature" T_t estimated from a "thermal" odd-even mass difference, while there is no sharp phase transition because of the finiteness of nucleus. It is found that T_t is in good agreement with predictions of critical temperature T_c in the BCS approximation, and the pairing correlations almost vanish at two points of the transition temperature $T \approx 2T_t$. The BCS calculations show that the critical temperature T_c increases with increasing deformation.

PACS: 21.60.Cs, 21.10.Ma, 05.30.-d

1 Introduction

Pairing correlations are one of the fundamental properties of nuclei. The odd-even mass difference observed in nuclear masses, and the energy gap of even-even nuclei are well known as signatures of pairing effects [1]. The Bardeen-Cooper-Schriffer (BCS) theory [2] of superconductivity has been applied to such nuclear problems at zero temperature [3]. The thermodynamical properties of nuclear pairing were investigated using the BCS theory in the study of hot nuclei [4,5]. Breaking of the Cooper pairs is expected to occur above a certain critical temperature. Infinite Fermi systems show a sharp phase transition from a super-fluid phase to a normal-fluid one at a critical temperature T_c, where the pairing gap vanishes and the heat capacity exhibits a singularity. For metal superconductors, the critical temperature is $T_c \approx 0.57\Delta$ MeV [2], where the pairing gap Δ is calculated using the BCS equation. In this case, we can image a well deformed nucleus for which level density is almost uniform and average level spacing is very small compared with the pairing gap Δ ($\approx$

1 MeV for the rare earth nuclei) [6]. On the other hand, the pairing correlations vanish at $T_c \approx 0.50\Delta$ MeV [7] in a simple pairing model with half-filled degenerate shells.

However in the case of the finite Fermi system like a nucleus, since the nuclear radius is much smaller than the coherence length of the Cooper pair, statistical fluctuations beyond the mean field become larger. The fluctuations smooth out the sharp phase transition, and then the pairing correlations do not vanish but decrease with increasing temperature. There are many approaches for treating the fluctuations beyond the mean field. A signature of the pairing transition at finite temperature might be a peak of the heat capacity as a function of temperature [8]. In fact, it has recently been reported [9,10] that the canonical heat capacities extracted from observed level densities in ^{162}Dy, ^{166}Er and ^{172}Yb form an S shape around $T \approx 0.5$ MeV, which is interpreted as the breaking of nucleon Cooper pairs and the pairing transition because the critical temperature corresponds to $T_c \approx 0.57\Delta \approx 0.5$ MeV in the BCS theory. The odd-even effect that shows that the heat capacity of an odd-mass nucleus is smaller than those of the adjacent even-mass nuclei can be found around the critical temperature T_c.

The spherical shell model approaches could be more appropriate for describing various aspects of nuclear structure. The large fluctuations can be taken into account beyond the mean field in the shell model calculations. For the description of nuclear properties at higher temperatures, one needs a large model space. Recently the shell model Monte Carlo (SMMC) calculations have been performed with the pure pairing force [11] in a large model space, and with the pairing and multipole-multipole forces [12] in the $fp + g_{9/2}$ shell model space for the even- and odd-mass Fe isotopes. It was shown that the pairing correlations would be important only at low temperatures and at low excitation energies [11], and that the suppression of pairing correlations due to finite temperature appears as the S shape of the heat capacity around the temperature $T \sim 0.8$ MeV [12]. The model space was quite recently extended to examine the partition functions and the level densities up to the higher temperature $T = 4.0$ MeV using an independent-particle approximation [13] combined with the SMMC method.

This paper is organized as follows. In Section 2, we carry out the shell model calculations in the large model space ($sd + fp + s_{1/2}d_{5/2}$) using a spherical Woods-Saxon potential [14], where we adopt the independent-particle approximation [13] and combine it with the shell model calculations in the sd-shell, though there are no contributions from many-body correlations in the fp shell or from the coupling between the fp and sd shells. The pairing correlations within the heat capacity or "thermal" odd-even mass difference as a function of finite temperature are estimated, and a "transition temperature" T_t is introduced to explain the pairing transition. Then the definitive signatures

of the pairing transition are identified. The critical temperature T_c is also evaluated using the BCS calculations with the axially deformed Woods-Saxon potential and a pairing residual interaction in Section 3. We discuss the relations between the transition temperature T_t and the critical temperature T_c. The systematic behavior of the critical temperature T_c is examined over a wide range of nuclei. We discuss the effects of deformation on the critical temperature. Concluding remarks are given in Section 4.

2 Pairing transition in shell model calculations

We start from the canonical partition function defined by

$$Z(T) = \mathrm{Tr}(\mathrm{e}^{-H/T}) = \sum_{i=0}^{\infty} \mathrm{e}^{-E_i/T}, \tag{1}$$

where E_i is the energy of the ith eigenstate for the Hamiltonian H of a system. The large matrix of the Hamiltonian H is diagonalized to obtain all the eigenvalues E_i, and the partition function in the canonical ensemble is calculated from Eq. (1). Then, any thermodynamical quantities $O(T)$ can be evaluated from

$$O(T) = \langle O \rangle = \mathrm{Tr}(O\mathrm{e}^{-H/T})/Z(T), \tag{2}$$

where $\langle O \rangle$ stands for the average value of operator O over the range of eigenstates. For instance, the thermal energy is expressed as

$$E(Z,N,T) = \langle H \rangle = \sum_{i=0}^{\infty} E_i \mathrm{e}^{-E_i/T}/Z(T). \tag{3}$$

The heat capacity is then given by

$$C(Z,N,T) = \frac{\partial E(Z,N,T)}{\partial T}. \tag{4}$$

We now introduce the thermal odd-even mass difference for neutrons defined by the following three-point indicator:

$$\begin{aligned}\Delta_n^{(3)}(Z,N,T) = & \frac{(-1)^N}{2}[E(Z,N+1,T) \\ & -2E(Z,N,T) + E(Z,N-1,T)].\end{aligned} \tag{5}$$

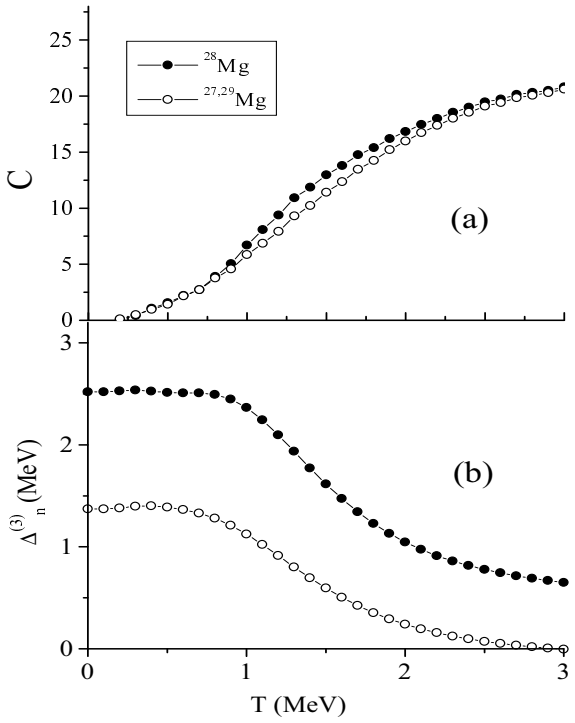

Fig. 1. Heat capacity (a) and thermal odd-even mass difference (b) as a function of temperature. The solid circles denote the values for even-even nucleus ^{28}Mg. The open circles denote the average values of the neighboring odd nuclei ^{27}Mg and ^{29}Mg.

The odd-even mass difference at zero temperature is known theoretically and experimentally as an important quantity in evaluation of the pairing correlations in a nucleus. The thermal odd-even mass difference is also an indicator of the pairing correlations at finite temperature, and can be obtained from the experimental energies and the level density as well as the heat capacity.

We now calculate the heat capacity (4) and the thermal odd-even mass difference (5) for $^{20-26}$Ne and $^{24-32}$Mg in the large model space ($sd + fp + s_{1/2}d_{5/2}$) using an independent-particle approximation [13]. The Woods-Saxon potential plus a spin-orbit interaction is diagonalized in a basis of harmonic-oscillator (H.O.) eigenfunctions, and then the single-particle energies are obtained [14]. The Woods-Saxon parameters are chosen so as to reproduce the single-particle energies estimated from ^{17}O. A number of unbound states ($E > 0$) are obtained due to the expansion in a finite number of H.O. eigenfunctions. The resonances with narrow widths are important for neutron-rich nuclei such as ^{66}Cr. It was shown [13], however, that while the narrow resonances make an important contribution to the partition function, their width can be ignored. In this paper, we ignore the widths of resonances and the continuum states. We carried out the shell model calculations in the *sd*-shell model space using the USD interaction [15], and calculated the correlated thermal energy $E_{v,tr}$ using Eq. (3). An enhancement of the heat capacity was found in even Mg

nuclei around $T \sim 1.5$ MeV. This enhancement is interpreted as a reduction in the pairing correlations. However, because the calculation was restricted to a finite space (*sd* shell), the calculated heat capacity reached its maximum around temperatures of ~ 1.5 MeV. Therefore, we extended the model space to sd+fp+$s_{1/2}d_{5/2}$ to display a much broader temperature range (~ 3.5 MeV). We combine the small model space *sd* of interaction effects with a large-space calculation of the independent-particle thermal energy E_{sp} as follows [13]:

$$E = E_{v,tr} + E_{sp} - E_{sp,tr}, \tag{6}$$

where $E_{sp,tr}$ is the independent-particle thermal energy in the *sd* space. Then the heat capacity and the thermal odd-even mass difference are obtained using Eqs. (4) and (5), respectively. As typical examples, the heat capacity and the thermal odd-even mass difference in $^{27-29}$Mg are plotted in Fig. 1 (a) and (b), where the average values of ^{27}Mg and ^{29}Mg are shown for odd-mass nuclei. The heat capacity $C(^{28}\mathrm{Mg})$ is larger than the average value $C(^{27,29}\mathrm{Mg}) = [C(^{27}\mathrm{Mg}) + C(^{29}\mathrm{Mg})]/2$ in $T = 0.8 - 3.0$ MeV, although it does not reach a peak. In other nuclei, we also found an odd-even effect where the average heat capacity of odd-mass nuclei is significantly lower than that of the adjacent even-mass nucleus. In Fig. 1 (a), one can see that with the usual relation $C = 2aT$ the parameter a has roughly the empirical value of $A/8$ MeV^{-1} [16] for light nuclei, and is considerably larger than the Fermi-gas model value $A/15$ MeV^{-1}. Figure 1 (b) shows the thermal odd-even mass difference defined by Eq. (5) for ^{28}Mg and ^{27,29}Mg. We find a gradual decrease of the thermal odd-even mass difference as a function of temperature, which is interpreted as a gradual breaking of nucleon Cooper pairs and the decline of pairing correlations. Figure 1 (b) also displays that $\Delta_n^{(3)}(^{28}\mathrm{Mg})$ is larger than $\Delta_n^{(3)}(^{27,29}\mathrm{Mg}) = [\Delta_n^{(3)}(^{27}\mathrm{Mg}) + \Delta_n^{(3)}(^{29}\mathrm{Mg})]/2$. At zero temperature, this is well known as the odd-even staggering of binding energies, which reflects the stronger binding of even-particle-number systems than the odd-particle-number neighbors [17,18]. Their analyses demonstrated that the odd-even mass difference for odd-particle number is an excellent measure of pairing correlations, although it is still controversial [19]. The symmetric filter $\delta e = 2\Delta_n^{(3)}(2m) - \Delta_n^{(3)}(2m-1) - \Delta_n^{(3)}(2m+1)$ extracts the effective single-particle spacing from the measured binding energies of deformed nuclei. We can see that the difference, $\delta e/2$, between $\Delta_n^{(3)}(^{28}\mathrm{Mg})$ and $\Delta_n^{(3)}(^{27,29}\mathrm{Mg})$ decreases gradually as temperature increases. This means that the effective single-particle spacing decreases as temperature increases. As one can see in Fig. 1 (b), $\Delta_n^{(3)}(^{27,29}\mathrm{Mg})$ is almost zero at $T \approx 3.0$ MeV, and the pairing correlations vanish at two points on the transition temperature T_t. On the other hand, $\Delta_n^{(3)}(^{28}\mathrm{Mg})$ still remains at this temperature. We now identify an inflection point of the curve $\Delta_n^{(3)}(^{27,29}\mathrm{Mg})$ in Fig. 1 (b) as a signature of pairing transition, and call it "transition temperature" T_t. To see more precise position of the inflection point, we differentiate $\Delta_n^{(3)}(^{27,29}\mathrm{Mg})$ with respect to

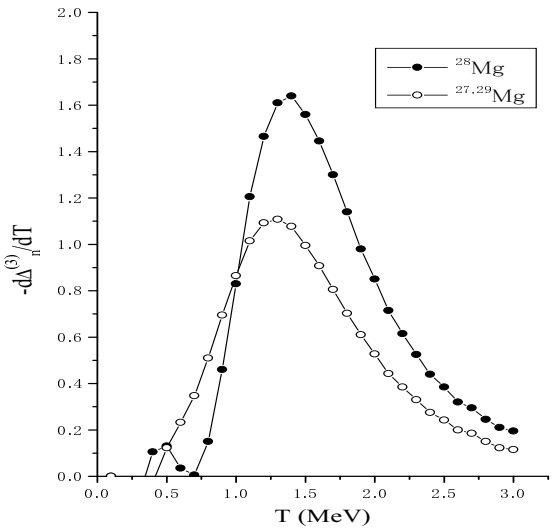

Fig. 2. Derivative of the thermal odd-even mass difference.

temperature T. As seen in Fig. 2, $-\partial\Delta_n^{(3)}(^{27,29}\mathrm{Mg})/\partial T$ has a peak at temperature $T_c \approx 1.3$ MeV corresponding to the transition temperature T_t, and the transition temperature T_t for ^{27,29}Mg is quite close to that for ^{28}Mg. It is very important to note that the difference between the two curves of the heat capacities in Fig. 1 (a) is equal to $-\partial\Delta_n^{(3)}(^{28}\mathrm{Mg})/\partial T$

$$-\frac{\partial\Delta_n^{(3)}(Z,N,T)}{\partial T} = (-1)^N\{C(Z,N,T) - \frac{1}{2}[C(Z,N+1,T) + C(Z,N-1,T)]\}. \quad (7)$$

Thus, the thermal odd-even mass difference is a good indicator for the pairing transition at the transition temperature estimated from a peak of $-\partial\Delta_n^{(3)}/\partial T$. It is important to note that the position of the peak does not change upon extension of the model space in the independent-particle approximation, which is different from the result of Ref. [11].

3 BCS calculations

In infinite systems, the BCS critical temperature is known to be proportional to the pairing gap $T_c = 0.57\Delta$. However, the relation is not axiomatic in a finite system like a nucleus. It seems that the peaks of the S-shaped heat capacities in ^{162}Dy, ^{166}Er, and ^{172}Yb correspond to the critical temperature $T_c = 0.57\Delta$ in the BCS prediction for infinite systems. It is therefore interesting to examine the correspondence using the BCS calculations over a wide range of nuclei. In

the BCS approximation, the pair gap Δ at finite temperature is obtained by using the following gap equation

$$1 = G \sum_{k>0} \frac{1-2f_k}{E_k}, \tag{8}$$

where ε_k are the single-particle energies, $E_k = \sqrt{(\varepsilon_k - \mu)^2 + \Delta^2}$ the quasiparticle energies, and $f_k = (1+\mathrm{e}^{E_k/T})^{-1}$ the Fermi-Dirac quasiparticle occupancies. The chemical potential μ is determined by the number constraint

$$N = \sum_{k>0} [1 - \frac{\varepsilon_k - \mu}{E_k}(1-2f_k)], \tag{9}$$

where the pairing force strength G is chosen so as to reproduce the experimental odd-even mass difference at zero temperature. In this calculation, we use the single-particle energies extracted from an axially deformed Woods-Saxon potential with spin-orbit interaction [14]. We chose the parameters so as to accommodate experimental single-particle energies extracted from energy levels of odd nucleus with double-closed core plus one neutron, i.e., ^{41}Ca, ^{101}Sn, and ^{209}Pb. The deformation takes into account the effects of a quadrupole-quadrupole interaction in the mean-field approximation. The deformation parameter in even-even nuclei can be estimated from $B(E2) = [(3/4\pi)Zer_0^2 A^{2/3}\beta]^2$ using experimental $B(E2)$ values. If they are not available, we adopt the empirical formula $B(E2) \approx 3.27 E_{2_1^+}^{-1.0} Z^2 A^{-0.69}$ for the

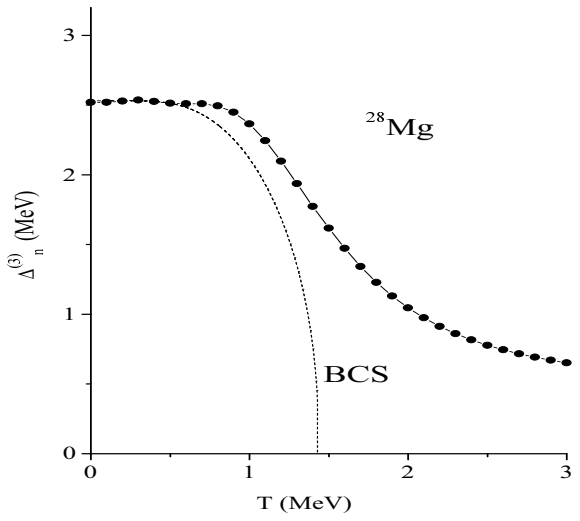

Fig. 3. Thermal odd-even mass difference. The solid circles represent the even-even nucleus ^{28}Mg, and the dotted line the pairing gap in the BCS approximation.

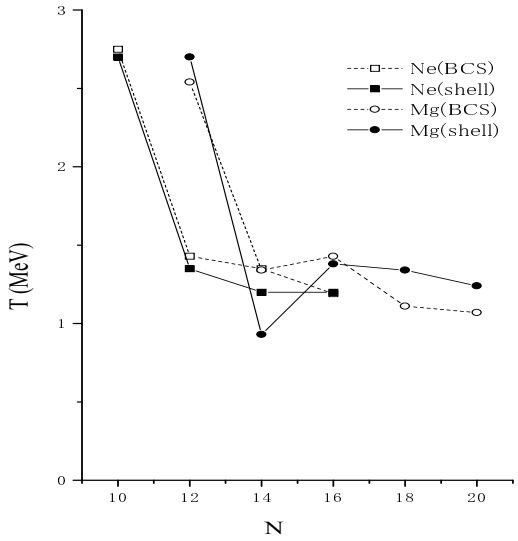

Fig. 4. Transition temperature T_t (solid symbols) and critical temperature T_c (open symbols) as a function of neutron number in the Ne and Mg isotopes.

$B(E2)$ values where $E_{2_1^+}$ is the energy of first excited 2^+ state in even-even nucleus. The number of two-fold degenerate active orbitals is chosen as 20 corresponding to N=2,3 shells above ^{40}Ca core in *sd*-nuclei, and 20 corresponding to N=3,4 shells above ^{100}Sn core in *fp*-nuclei for each proton and neutron. For heavy nuclei, the numbers of active proton and neutron orbitals are taken as 30 corresponding to N=4,5 and N=5,6 shells above ^{208}Pb core, respectively. The BCS pairing gap for ^{28}Mg is shown in Fig. 3. The value of $\Delta_n^{(3)}$ decreases with increasing temperature, and vanishes at $T_c \approx 1.4$ MeV for ^{28}Mg. We can see that the critical temperature for ^{28}Mg is very close to the peak of the heat capacity.

For the Ne and Mg isotopes examined, we examine the temperature about the peak of $-\partial\Delta_n^{(3)}/\partial T$ in the shell model calculation and the critical temperature T_c in the BCS. Figure 4 suggests that the critical temperature T_c can be identified with the transition temperature T_t even though the pairing correlations do not vanish. It is very important to note that the $N = Z$ nuclei ^{20}Ne, ^{24}Mg show a high transition temperature $T_t \approx 2.7$ MeV, while the other $N > Z$ nuclei have $T_t \approx 1.3$ MeV. In our previous paper [20], we suggested that proton-neutron (p-n) correlations give rise to large odd-even mass difference in $N = Z$ nuclei. The cooperation of the p-n pairing correlations with the like-nucleon correlations would increase the transition temperature as well.

We have found correspondence between the "transition temperature" and the BCS critical temperature in light nuclei. It is worth examining whether or not the correspondence obtained in light nuclei also holds in heavy nuclei over a wide range. Carrying out exact shell-model calculations is, however,

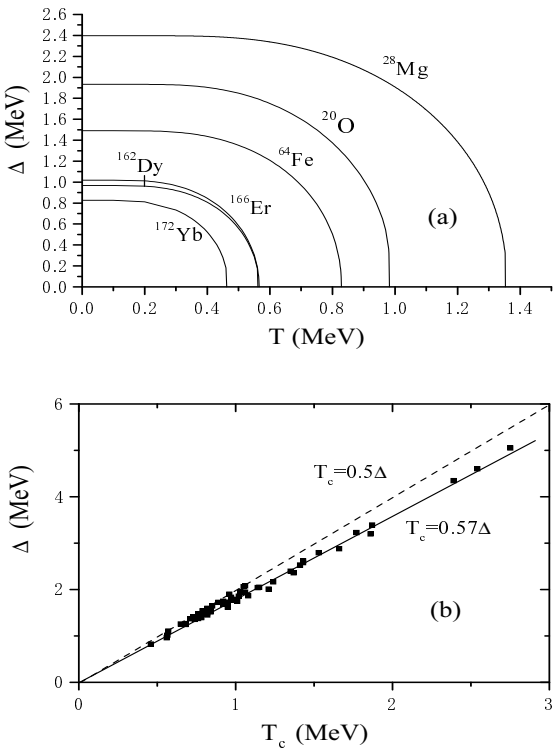

Fig. 5. The upper graph (a) shows the neutron pairing gap Δ versus temperature T. The lower graph (b) shows the neutron pairing gap at zero temperature versus the critical temperature T_c in the BCS calculation.

possible only for light nuclei but not for heavy nuclei. We apply the "correspondence formula" found in the BCS approximation for the Mg and Ne isotopes to heavy nuclei. Since the transition temperature T_t can be regarded as the critical temperature T_c from the above discussions, it is now interesting to investigate the neutron gap and the critical temperature in the BCS calculation solving the gap equation (8) with the number equation (9) over a wide range of even-even nuclei, i.e., ^{20,22}O, $^{20-26}$Ne, $^{24-32}$Mg, $^{28-32}$Si, $^{32-38}$S, $^{36-40}$Ar, $^{42-46}$Ca, $^{44-48}$Ti, $^{48-52}$Cr, $^{54-66}$Fe, $^{104-124}$Sn, $^{108-114}$Te, ^{124,130}Ce, ^{132}Nd, ^{134}Sm, ^{140,144,154}Gd, ^{162}Dy, ^{166}Er, and ^{172}Yb. The pairing force strength G is determined so as to reproduce the experimental odd-even mass difference at zero temperature. The neutron pairing gap vanishes at the critical temperature for each nuclei as seen in the upper graph (a) of Fig. 5. The critical temperatures of ^{162}Dy, ^{166}Er, and ^{172}Yb are around $T_c \approx 0.5$ MeV, which corresponds to the peak of the experimental heat capacity [9,10]. In addition, the critical temperature $T_c \sim 0.8$ MeV for ^{64}Fe agrees with the temperature of peak in the heat capacity obtained using the SMMC calculations [11,12]. These results support the conjecture that the pairing transition temperature T_t corresponds to the critical temperature T_c. In the lower graph (b) of Fig. 5, the neutron gaps at zero temperature are plotted as a function of T_c and the two lines are denoted as a guide eye. One is the line $T_c \approx 0.57\Delta$ derived from the BCS theory [2]. The other is that of a simple pairing model with half-filled degenerate shells,

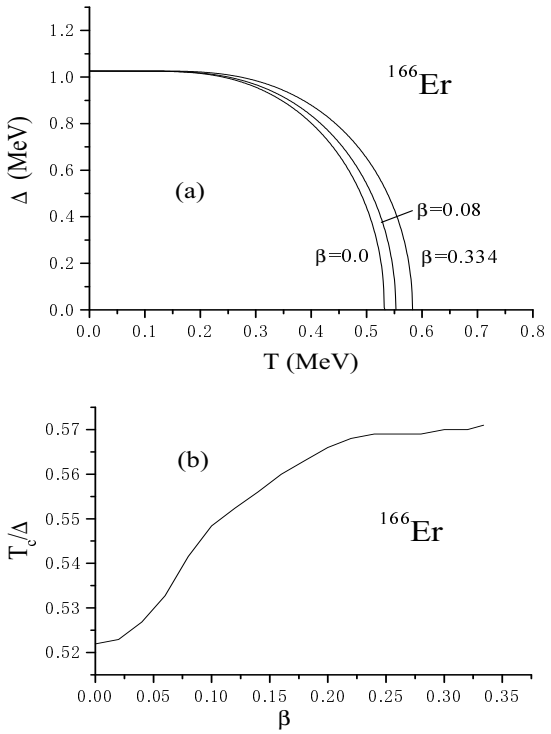

Fig. 6. Deformation dependence of the critical temperature T_c in the BCS calculation. The upper graph (a) shows the neutron gap in β=0.0, 0.08, and 0.334. The lower graph (b) shows the ratio of the critical temperature T_c and the gap Δ_n.

where the pairing gaps vanish at $T_c \approx 0.50\Delta$ MeV [7]. Almost all the plots lie between these two lines, and those for deformed nuclei are very close to the line $T_c = 0.57\Delta$. For instance, the critical temperature of ^{166}Er exhibits $T_c = 0.58$ MeV where Δ=1.02 MeV and the deformation β=0.334. Since a well deformed nucleus can be regarded as a system with almost uniform level density and a small average level spacing compared with the gap Δ (≈ 1 MeV for the rare earth nuclei) [6], this result is reasonable. This is simply the case for the metal superconductors. The critical temperature is given by $T_c \sim 0.57\Delta$ ($\Delta = \omega e^{-1/\rho G}$) where ω is the phonon energy and ρ the average level density at the Fermi surface, and T_c is sensitive to the level density. On the other hand, the simple pairing model with half-filled degenerate shells leads to $T_c \approx 0.50\Delta$ MeV [7]. Thus it seems that the critical temperature depends on the degree of deformation. In fact, Fig. 6 shows that the critical temperature T_c increases with increasing deformation in ^{166}Er.

4 Concluding remarks

In conclusion, we have studied the pairing transition at finite temperature using the shell model calculations. We have demonstrated that the thermal

odd-even mass difference is a good indicator for the pairing transition at finite temperature as well as the usual one at zero temperature. We suggest that the pairing correlations can be estimated from the measured level densities of nuclei with neutron number $N+1$, N, and $N-1$, for instance, ^{170}Yb, ^{171}Yb, and ^{172}Yb. It was shown that the transition temperature T_t corresponding to the inflection point of the curve $\Delta_n^{(3)}$ is almost identical to the critical temperature T_c in the BCS method. The pairing correlations almost vanish at two points on the transition temperature T_t. The critical temperature T_c depends on the deformation of a nucleus, and increases with increasing deformation. The critical temperature T_c of deformed nuclei follows $T_c \approx 0.57\Delta$ MeV as the case of the metal superconductors. The transition temperature in the case of $N = Z$ nuclei is comparatively higher than those of the neighboring $N > Z$ nuclei. The p-n pair correlations seems to contribute to the increase of the transition temperature. In addition, as the p-n pairing is crucial for formation of an α-like correlated structure in the $N = Z$ nuclei [21], we can expect the breaking of p-n pairs as well as like-nucleon pairs at a certain temperature. Further studies in this direction are in progress.

References

[1] A. Bohr, B. R. Mottelson, and D. Pines, Phys. Rev. **110** (1958) 936.

[2] J. Bardeen, L. N. Cooper, and J. R. Schrieffer, Phys. Rev. **108** (1957) 1175.

[3] S. T. Belyaev, Mat. Fys. Medd. Dan. Vid. Selsk. **31**, No. 11(1959).

[4] M. Sano and S. Yamasaki, Prog. Theor. Phys. **29** (1963) 397.

[5] A. L. Goodman, Nucl. Phys. **A352** (1981) 45.

[6] P. Ring and Schuck, 'Text book', (1981).

[7] A. L. Goodman, Nucl. Phys. A 352 (1981) 30; Nucl. Phys. A 352 (1981) 45.

[8] R. Rossignoli, N. Canosa, and P. Ring, Phys. Rev. Lett. **80** (1998) 1853.

[9] A. Schiller, A. Bierve, M. Guttormsen, M. Hjorth-Jensen, F. Ingebretsen, E. Melby, S. Messelt, J. Rekstad, S. Siem, and S. W. Ødegard, Phys. Rev. C **63** (2001) 021306R.

[10] E. Melby, L. Bergholt, M. Guttormsen, M. Hjorth-Jensen, F. Ingebretsen, S. Messelt, J. Rekstad, A. Schiller, S. Siem, and S. W. Ødegard, Phys. Rev. Lett. **83** (1999) 3510.

[11] S. Rombouts, K. Heyde, and N. Jachowicz, Phys. Rev. C **58** (1998) 3295.

[12] S. Liu and Y. Alhassid, Phys. Rev. Lett. **87** (2001) 022501.

[13] Y. Alhassid, G. F. Bertsch, and L. Fang, Phys. Rev. C **68** (2003) 044322.

[14] S. Cwoik, J. Dudek, W. Nazarewicz, J. Skalski, and T. Werner, Comput. Phys. Commun. **46** (1987) 379.

[15] B. A. Brown and B. H. Wildenthal, Annu. Rev. Phys. Part. Sci. **38** (1988) 29.

[16] A. Bohr and B. R. Mottelson, Nuclear Structure, Vol 1 (Benjamin, NY, 1969).

[17] W. Satula, J. Dobaczewski, and W. Nazarewicz, Phys. Rev. Lett. **81** (1998) 3599.

[18] J. Dobaczewski, P. Magierski, W. Nazarewicz, W. Satula, and Z. Szymański, Phys. Rev. C **63** (2001) 024308.

[19] T. Duguet, P. Bonche, P.-H. Heenen, and J. Meyer, Phys. Rev. C **65** (2001) 014311.

[20] K. Kaneko and M. Hasegawa, Phys. Rev. C **60** (1999) 024301.

[21] M. Hasegawa and K. Kaneko, Phys. Rev. C **61** (2000) 037306.